

RSC Advances



This is an *Accepted Manuscript*, which has been through the Royal Society of Chemistry peer review process and has been accepted for publication.

Accepted Manuscripts are published online shortly after acceptance, before technical editing, formatting and proof reading. Using this free service, authors can make their results available to the community, in citable form, before we publish the edited article. This *Accepted Manuscript* will be replaced by the edited, formatted and paginated article as soon as this is available.

You can find more information about *Accepted Manuscripts* in the [Information for Authors](#).

Please note that technical editing may introduce minor changes to the text and/or graphics, which may alter content. The journal's standard [Terms & Conditions](#) and the [Ethical guidelines](#) still apply. In no event shall the Royal Society of Chemistry be held responsible for any errors or omissions in this *Accepted Manuscript* or any consequences arising from the use of any information it contains.

ARTICLE

Ruthenium complexes as inhibitors of human islet amyloid polypeptide aggregation, an effect that prevents beta cell apoptosis

Cite this: DOI: 10.1039/x0xx00000x

Lijuan Ma[#], Yuanting Fu[#], Lianling Yu, Xiaoling Li^{*}, Wenjie Zheng, Tianfeng Chen^{*}Received 00th January 2012,
Accepted 00th January 2012

DOI: 10.1039/x0xx00000x

www.rsc.org/

Human islet amyloid polypeptide (hIAPP) aggregation are essential in the loss of insulin-producing pancreatic beta cells in type 2 diabetes mellitus (T2DM). Recent studies have identified hIAPP fibril as therapeutic target of T2DM. Metal complexes could covalently bind to the intracellular peptides to regulate their biological functions. In the present study, ruthenium (Ru) complexes NAMI-A (**1**), [Ru(bpy)₃](ClO₄)₂ (**2**) (bpy = 2,2'-dipyridyl), [Ru(pip)₃](ClO₄)₂ (**3**) (pip = 2-phenylimidazo[4,5-f]-[1,10]phenanthroline) and [Ru(phtpy)(phen)Cl]ClO₄ (**4**) (phtpy = 2,6-bis(2-pyridyl)-4-phenylpyridine, phen = 1,10-phenanthroline) were selected to investigate their influence on hIAPP fibrillation *in vitro*. The results of thioflavin T (ThT) fluorescence assay showed that, Ru complexes effectively inhibited the formation of hIAPP fibril. AFM images and TEM images further validated that the hIAPP fibrillation was disaggregation by the Ru complexes, and then to form nanoscale particles, which tends to be a time-dependent process. Moreover, Ru complexes demonstrated protective effect towards hIAPP-caused cell damage by restraining ROS generation and blocking cell apoptosis. Meantime, it has been found that Ru complexes can also disaggregate hIAPP fibrils effectively inside the cells, and the effects were proportional to the lipophilicity of complexes. Taken together, this study provides a strategy for design of Ru complexes for treatment of T2DM by targeting hIAPP.

INTRODUCTION

Cancer Amyloid-related diseases like Alzheimer's disease (AD) with amyloid- β peptide (A β), spongiform encephalopathies with prion protein (PrP) and type 2 diabetes mellitus (T2DM) with islet amyloid polypeptide (IAPP), as well as other degenerative diseases, are characterized by protein conformational change and amyloid fibril formation¹⁻³. Therein, human islet amyloid polypeptide (hIAPP, also known as human amylin) is a 37-amino-acid peptide synthesized in pancreatic beta cells and co-secreted along with insulin in response to beta cell secretagogues, which is demonstrated easy to aggregate and form amyloid fibril deposits, inducing the dysfunction and death of pancreatic β -cell in the pathology of T2DM⁴⁻⁸. Whereas, the misfolding and amyloid fibril formation of hIAPP, which undergo conformational transition of a random coil into the β -sheet, are cytotoxic in a disease state^{9, 10}. Evidence has suggested that the toxicity of hIAPP fibril formation is very likely to be correlated with membrane disruption^{11, 12}. Oxidative stress and ion-permeable channels are thought to be the toxicity mechanisms¹³⁻¹⁵, but this argument is controversial. Thus, the exact mechanism of toxicity induced by hIAPP aggregation remains elusive.

Considering the toxicity of hIAPP aggregates, a variety of inhibitors towards hIAPP aggregation, such as peptide-based

inhibitors, coordination compounds and small molecule inhibitors¹⁶⁻¹⁸, is developed. It is reported that several metal ions could inhibit hIAPP fibril formation effectively¹⁹. Ward et al discovered Cu (II) prevents hIAPP from forming the β -sheet conformers through its destabilisation of the intramolecular disulphide bridge, Al (III) and Zn (II) significantly increase the formation of hIAPP fibrils, and Fe (III) appears to have the least influence upon the hIAPP aggregation²⁰. Besides, The metal complexes which could covalently bound to the corresponding peptide would be a promising drug for inhibiting amyloid fibril formation²¹. Lee et al designed a Co (III) complex as peptide-cleavage agent to cleave the oligomers of hIAPP and inhibit the apoptosis of INS-1 cell induced by hIAPP even in the presence of polymeric aggregate of hIAPP²². Similarly, cleavage agent of Cu (II) cyclen obtained estimated 8.3 mol % cleavage yield of β -sheet conformers¹⁷. Vyas et al synthesized two ruthenium (Ru) polypyridyl complexes that could efficiently inhibit A β (1-40) aggregation and were non-toxic to human neuroblastoma cells, whose ancillary ligand plays significant role in the A β inhibitory potency²³. Since A β and hIAPP are both inclined to form fibrous deposition, Ru complexes were also found could inhibit amylin from forming β -sheets and promote the disaggregation of the amyloidogenesis by remarkably changing the β -sheet

components²⁴. However, little information about the interaction between Ru complexes and hIAPP is available.

Ru complexes offer several advantages like feasible synthesis, inertness to substitution, stability in biological environment, expansions of functional groups by variation in surrounding ligands and inherent photophysical properties^{25, 26}. Till now, several Ru complexes have been proposed as anti-cancer drug leads. However, studies also reported the toxicity of Ru complexes against different cell lines^{27, 28}. Therefore, rational design of biological active Ru complexes with low toxicity and hIAPP-inhibitory effects has kindled great interest of scientists from the fields of chemistry and medicine. In the present study, a series of Ru complexes, including NAMI-A (**1**) [Ru(bpy)₃](ClO₄)₂ (**2**), [Ru(pip)₃](ClO₄)₂ (**3**) and [Ru(phtpy)(phen)Cl]ClO₄ (**4**) were synthesized and selected to investigate their interaction with hIAPP. The results of extracellular and *in vitro* cell studies both provided strong evidence of the inhibition of Ru complexes on the amyloid fibrillation of hIAPP, and thus prevent the beta cell apoptosis, which demonstrate that Ru complexes could bind hIAPP and alter its physicochemical properties to inhibit the cellular toxicity. Taken together, this study provides a strategy for design of Ru complexes for treatment of T2DM by targeting hIAPP.

EXPERIMENTAL SECTIONS

Materials and Chemicals

Human islet amyloid polypeptide (hIAPP), RuCl₃•3H₂O, NaClO₄, ligands 2,2'-bipyridine(bpy), 2-phenylimidazo[4,5-f][1,10]phenanthroline(pip), 2,6-Bis(2-pyridyl)-4-phenylpyridine (phtpy) and 1,10-phenanthroline (phen) were purchased commercially and used without further purification. Thioflavin T (ThT) was purchased from Shanghai Godo Industrial Co., Ltd. H₂DCF-DA, dihydroethidium (DHE), bicinchoninic acid (BCA) protein assay kit, substrates for caspase-3 (Ac-DEVD-AMC), caspase-8 (Ac-IETD-AMC) and caspase-9 (Ac-LEHDAMC) were purchased from Sigma-Aldrich.

Synthesis of the Ru complexes

In the present study, complexes **1**, **2**, **3** and **4** were synthesized and characterized as previously reported with slight modification²⁸⁻³⁰.

Tyrosine intrinsic fluorescence assay

10 μM hIAPP solution was incubated alone or in the presence of 5 μM complexes **1**, **2**, **3** and **4** for 48 h at 37 °C. Two group were carried out, one group were incubated in normal light room and the other were incubated in the dark room. And different concentration of the **3** were incubated 10 μM hIAPP for 48 h at 37 °C. Respectively. Samples were placed in a four-sided quartz fluorescence cuvette and data were recorded at indicated time. Fluorescence spectra were collected using a F-4500 FL Spectrophotometer (Hitachi, Japan). Ex= 280 nm (slit width = 5 nm), and emission (slit width = 10 nm) was monitored over 290-400 nm.

Thioflavin T (ThT) fluorescence assay

10 μM hIAPP was incubated with or without 5 μM complexes **1**, **2**, **3** and **4** solution in PBS buffer (phosphate buffered saline, containing NaCl 137 mM, KCl 2.7 mM, Na₂HPO₄ 10 mM, KH₂PO₄ 2 mM, pH 7.4) for 48 h at 37 °C. 40 μl incubated solution and 160 μl ThT (50 μM) were added in 96 wells black microplate. Fluorescence measurements were observed by a spectrofluorometer (Spectra Max M5, Bio-Tek) at 37 °C. 440 nm and 482 nm was set as the excitation and emission wavelengths respectively.

Particle size analysis

The Particle size was measured by the Zetasizer Nano ZS particle analyzer (Malvern Instruments Limited)³¹. Briefly, 10 μM hIAPP in the absence and presence of 5 μM complexes **1**, **2**, **3** and **4** solution was incubated in PBS for 48 h at 37 °C. 1 ml mixed solution were extracted for measurement.

Particle size analysis by AFM and TEM

hIAPP samples were characterized by AFM and TEM²⁸. In brief, 10 μM hIAPP was incubated with or without 5 μM complexes **1**, **2**, **3** and **4** solution for 48 h at 37 °C. 10 μl incubated solution were obtained by a Bioscope Catylyst Nanoscope-V (Veeco instruments, USA) to get ATM images. The TEM images were visualized at Hitachi (H-7650) transmission electron microscope operating at 80 kV.

Cell culture and MTT assay

INS-1 rat insulinoma cell line was purchased from American Type Culture Collection (ATCC, Manassas, VA, USA). They were incubated in RPMI-1640 medium supplemented with 10% FBS, 10 mmol/L HEPES, 50 mmol/L mercaptoethanol, 2 mmol/L L-glutamine, 1 mmol/L sodium pyruvate, 100 U/ml penicillin and 100 mg/ml streptomycin at 37 °C in CO₂ incubator (95% relative humidity, 5% CO₂). Cell viability was determined by measuring by MTT assay as previously described^{32, 33}. 6×10⁴ INS-1 cells per well were seeded in 96-well tissue culture plates at 37 C for 24 h. Different concentrations of hIAPP and Ru complexes were added for another 48 h. Then, MTT solution was added to each well and incubated at 37 C for 4 h. The absorbance of the cells at 570 nm was determined by microplate reader (Spectra Max M5). all the experiments were carried out at least for three times, and the data were presented as averages of three independent experiments mean ± standard deviations.

Caspase activity assay.

Caspase activity was detected the fluorescence intensity with using specific caspase-3, -8, and -9 substrates. Briefly, after treated with 20 μM hIAPP alone or with 5 μM Ru complexes, the cell pellets were harvested and then suspended in cell lysis buffer for 2 h. Then the cell protein were obtain after centrifugation at 12 000 g for 20 min, after that, the cell lysates were placed in 96-well plates with caspase-3, -8, and -9 substrates to determined the fluorescence intensity with

microplate reader (Spectra Max M5, Bio-Tek) with ex/em wavelengths set at 380/460 nm.

Measurement of ROS generation

Intracellular ROS accumulation was evaluated by H₂DCF-DA assay and DHE assay according to an existing protocol^{34, 35}. Briefly, INS-1 cells at a density of 1×10^6 cells/mL were seeded in 96 wells plates, hIAPP (10 μ M) with or without different Ru complexes (5 μ M) were added, and incubated for 60 min. Subsequently, the cells were incubated with H₂DCF-DA (10 μ M) or DHE (10 μ M) at 37 °C for 30 min. The ROS level was then examined by the fluorescence intensity with microplate reader (Spectra Max M5) with ex/em wavelengths set at 488/525 nm for DCF and 300/600 nm for DHE probe.

Detection of Intracellular hIAPP Aggregation

Intracellular hIAPP aggregate detection was performed inside INS-1 cells. Briefly, cells were grown on cover glass in 6 wells plates, pretreated with 10 μ M hIAPP and 5 μ M Ru complexes for 48 h at room temperature. Subsequently, 4.0% paraformaldehyde were added and incubated for 10 min at 37 °C. After then, cells were cultured with 50 μ M ThT and DAPI (1 μ g \cdot mg⁻¹) for 30 min and washed twice with PBS and observed under a fluorescence microscope (Axiophot, Zeiss).

Measurement of Lipophilicity of Ru complexes

The lipophilicity of the Ru complexes was measured by using the “shake-flask” method as previously described³⁶. The concentrations of the Ru complexes in each phase were determined by UV-Vis analysis. The results were calculated by $\log P = \lg([\text{solute}]_{\text{octanol}} / [\text{solute}]_{\text{water}})$.

Interaction between hIAPP and Ru complexes

Briefly, 10 μ M of hIAPP were incubated with 5 μ M of Ru complex **3** for 48 h at 37 °C. After that, the mass spectra were obtained on a ABI4000 Q TRAP liquid chromatography-mass spectrometer (ABI, USA).

Statistics analysis

All experiments were carried out at least in triplicate, and the data are expressed as mean \pm standard deviation. Differences between the control and the experimental groups were analyzed by two-tailed Student's t test. One-way analysis of variance (ANOVA) was used in multiple group comparisons. Statistical analysis was performed using SPSS statistical program version 13 (SPSS Inc., Chicago, IL). Significant difference between treatment and control groups is indicated at * $P < 0.05$, ** $P < 0.01$ level.

RESULTS AND DISCUSSION

Ru complexes inhibit hIAPP fibrillation *in vitro*

As Ru polypyridyl complexes could efficiently inhibit A β (1-40) aggregation and demonstrated negligibly toxicity to human neuroblastoma cells²³, Ru complexes may showed several advantages in inhibit amyloid fibril formation. Herein, we

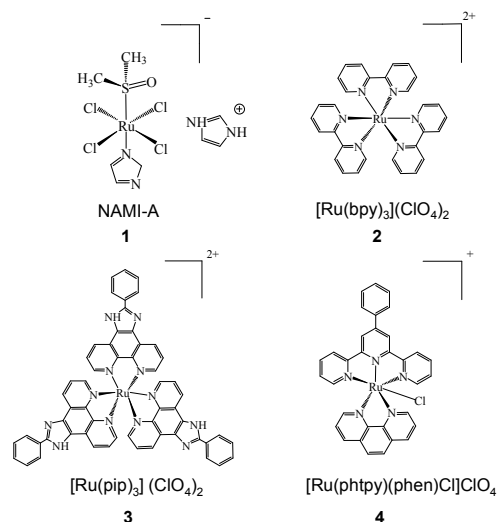


Figure 1. Chemical structures of Ru complexes in this study.

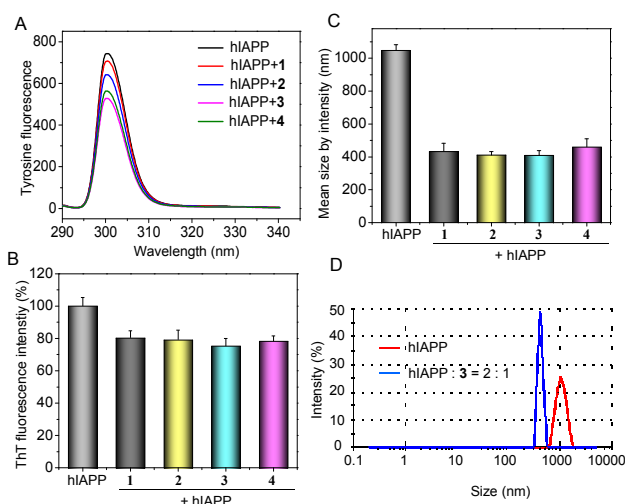


Figure 2. The influence of Ru complexes on hIAPP fibrillation. (A) The tyrosine fluorescence signal of 10 μ M hIAPP after treated with or without Ru complexes (5 μ M) in the normal light. (B) The intensity of ThT fluorescence signal of 10 μ M hIAPP after incubate with or without 5 μ M different Ru complexes for 48 h at 37 °C. The fluorescence signal were quenched after incubated with the complexes. (C) Size distribution of 10 μ M hIAPP incubated alone or with different complexes for 48 h at 37 °C characterized by intensity. (D) Size distribution of 10 μ M hIAPP incubated alone or with 5 μ M complex **3** for 48 h at 37 °C characterized by intensity.

selected different Ru complexes **1**, **2**, **3** and **4** to investigate their effect on the fibrillation of hIAPP (**Figure 1**). The change of the tyrosine fluorescence intensity was widely used to examine the interaction between the polypeptide and the Ru complexes. The tyrosine fluorescence of hIAPP would quench when a complex binds to the tyrosine. Many studies have examined the change in the tyrosine fluorescence intensity to confirm the interaction between hIAPP and Cu(II).^{20, 37, 38} Therefore, in this study, the tyrosine intrinsic fluorescence assay was chosen to detect the interaction between Ru

complexes and hIAPP. As a result, after hIAPP co-incubated with complexes **1**, **2**, **3** and **4** respectively, the tyrosine intrinsic fluorescence was quenched in the darkroom group (Figure S1) as well as in the normal light group (Figure 2A). These results indicate that the fluorescence quenching effects were not attributed to the photo-induced cross-linking of the peptide with the Ru complexes, but should be due to the interaction between Ru complexes and hIAPP. Furthermore, the fluorescence intensity was proportional to the concentration of **3**, which also confirmed the interaction between Ru complexes and hIAPP. Then, for in-depth exploration of the structural impact of Ru complexes on hIAPP, we take the thioflavin T (ThT) fluorescence assay, which is thought to be the effective method to detect amyloid fibril formation³⁹. The degree of amyloid fibril formation is associated with intensity of ThT fluorescence signal, which was thought to be proportional relationship. Through ThT assay (Figure 2B), we found that comparing with hIAPP group, ThT fluorescence signal was decreased after incubated with complexes **1**, **2**, **3** and **4** at pH 7.4 respectively, suggesting that Ru complexes could inhibit the formation of hIAPP fibril. Furthermore, the multimodal size distribution peaks of hIAPP after treatment with Ru complexes was revealed by the particle size analysis. The mean radius of hIAPP was more than 1000 nm after 48 h incubation, whereas the radius decreased dramatically after addition of Ru complexes (Figure 2C). Taking complex **3** as an example, hIAPP size obtained a minimum of less than 400 nm under the influence of complex **3**. Size distribution of hIAPP with or without complex **3** was intuitively showed in Figure 2D. The result of particle size analysis further confirmed that different Ru complexes could inhibit hIAPP aggregation *in vitro* respectively.

TEM images validated the changed morphology of hIAPP by complexes **1**, **2**, **3** and **4** visually. Herein, TEM and AFM images both showed that the fibrillation of hIAPP were

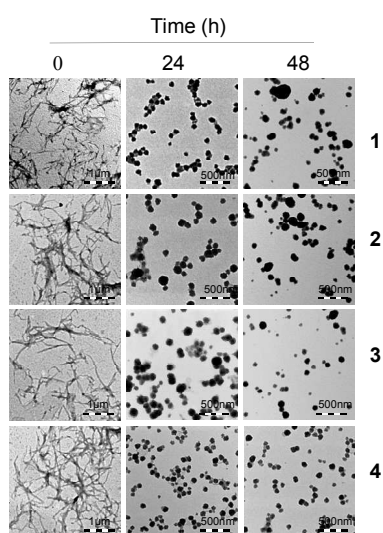


Figure 3. TEM images of time-dependent disaggregation of 10 μM hIAPP incubated with 5 μM different Ru complexes for 24 h or 48 h at 37 $^{\circ}\text{C}$.

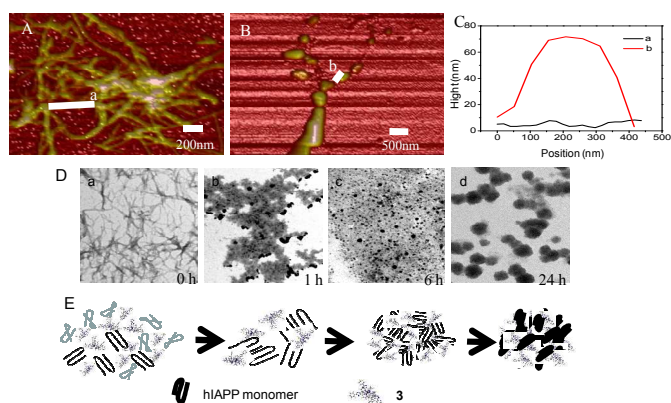


Figure 4. Complex **3** disaggregate hIAPP fibrils. AFM images of 10 μM hIAPP incubated alone (A), with 5 μM complex **3** (B) for 48 h at 37 $^{\circ}\text{C}$. (C) Height and position comparison of the fibril and granular aggregate along the line a and b. (D) TEM images of 10 μM hIAPP incubated (a) alone, (b-d) with 5 μM complex **3** for 1 h, 6 h and 24 h at 37 $^{\circ}\text{C}$ respectively. (E) Proposed schematic diagram of the mechanism of the disintegration of hIAPP amyloid fibril by the complex **3**.

appeared when incubated alone for 0 h or 48 h (Figure 3, Figure 4A). While when hIAPP incubated with 5 μM different Ru complexes, fibrillation was interrupted by them to form nanoscale granular particles. As showed in the Figure 3, slender and fibroid amyloid fibril were observed obviously at the beginning. While after 24 h of incubation, disaggregation of fibril were clear to show, the long fibroid hIAPP have disaggregated to many shortened fibrils and appearing some spherical particles. After 48 h of incubation, there were no visible fibrils, moreover, the most of previous shortened fibrils were disaggregated and changed into different degrees of spherical particles. Compared with other complexes, the complex **3** incubated with hIAPP presented a thorough disaggregation with the appeared dispersive and small spherical particles, demonstrating the fibrils were completely disaggregated into spherical particles. To investigate the complex **3** potential for fibril disaggregation, the individual AFM and TEM images were performed (Figure 4). hIAPP could form fibrils during incubation alone (Figure 4A), while nanoscale oligomers were formed when the peptides were incubated with complex **3** for 48 h (Figure 4B). Figure 4C demonstrated the surface morphology of line a and line b, which demonstrate the difference between smooth hIAPP fibril and granular particles. Complex **3** blocked the formation of hIAPP oligomers to form small particles, which continued to grow into nano size particles in 24 h (Figure 4D). The inhibition of Ru complexes on the hIAPP fibrillation was also revealed by a time-course study. The potential mechanism of the time-dependent disintegration of hIAPP fibril by the complex **3** was proposed in Figure 4E. These results were in accordance with tyrosine intrinsic fluorescence assay, ThT fluorescence assay and particle size analysis. It proved that the amyloid fibril formation was restrained by Ru complexes, which tended to form granular particles.

Furthermore, mass spectrometry was used to examine the chemical interaction between the hIAPP and the Ru complexes.

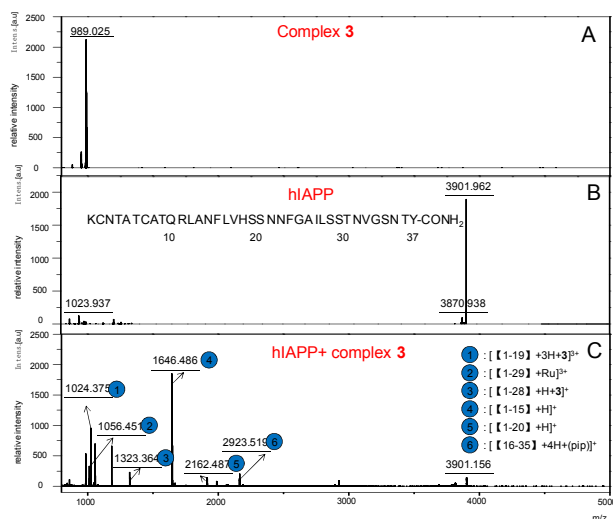


Figure 5. Interaction of the hIAPP with complex 3. MALDI-TOF-MS analysis of the 5 μM complex 3 (A), 10 μM hIAPP (B) and the mixed-solution of complex 3 and hIAPP (C) after incubation for 48 h at 37 $^{\circ}\text{C}$

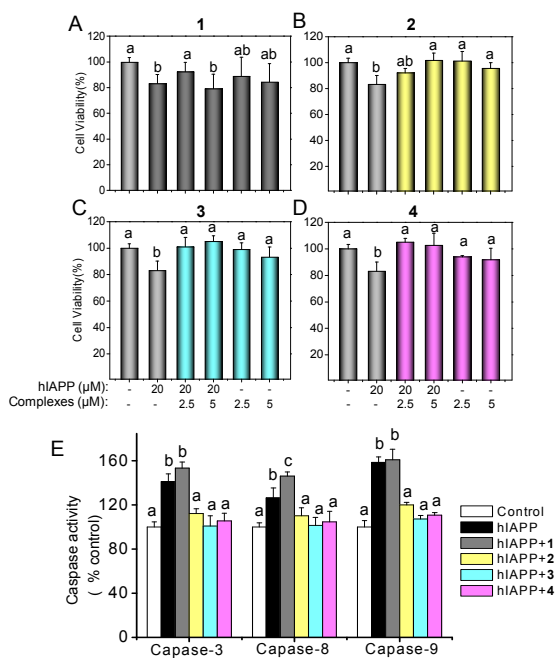


Figure 6. Ru complexes inhibit hIAPP-induced cell cytotoxicity and apoptosis. The cells were treated with 20 μM hIAPP in combination with different concentrations of complexes 1(A), 2(B), 3(C) and 4(D) at 37 $^{\circ}\text{C}$ for 48 h. (E) The caspase activities in cells treated with hIAPP were suppressed by the Ru complexes. INS-1 cells were pretreated with hIAPP (10 μM) and Ru complexes (5 μM) for 48 h as described in experiment section. Caspase activities were measured by synthetic fluorogenic substrate. Bars with different characters are statistically different at $P < 0.05$ level as analyzed by one-way ANOVA multiple comparison.

As shown in **Figure 5**, sharp peaks were observed in the spectra of complex 3 and hIAPP alone. After the incubation, new peaks were observed, indicating the binding and interaction between complex 3 and hIAPP. Detailed analysis of the peaks revealed the binding sequences of the peptides with the Ru complexes.

Ru complexes inhibit hIAPP-induced cell apoptosis

Misfolded hIAPP fibrillating is known as crucial reason in the pathogenesis of T2DM, leading to the death of islet beta cells⁴⁰. As the Ru complexes could inhibit hIAPP fibrillation and disaggregate hIAPP amyloid fibril into nanoscale particles in PBS buffer, whether the Ru complexes could disaggregate hIAPP fibrils in cells is indeterminable. Therefore, we select INS-1 cells as a pattern to examine whether the disaggregation is still exist. Herein, the cytotoxicity of hIAPP on cultured INS-1 cells in the absence and presence of complexes 1, 2, 3 and 4 were measured by the MTT assay. As showed in **Figure 6A-D**, the INS-1 cells viability were reduced after cultured with 20 μM hIAPP alone, while in presence of different concentration of Ru complexes, the reduction of cells viability was suppressed, except for the complex 1. As showed in **Figure 6A**, after co-treated with 5 μM complex 1 the hIAPP showed higher toxicity in the INS-1 cells, which was indicated that complex 1 will induced cell death in the concentration of 5 μM . In the other hand, these results indicated that most of Ru complexes could inhibit hIAPP-induced beta cell death effectively. Take complex 3 for instance, the viability of the cells treated with hIAPP alone was only 83.2%, while after the hIAPP incubated with complex 3, the cell viability increased into 101.1% and 105.2% (**Figure 6C**), indicating that complex 3 not only weakened the cell cytotoxicity of hIAPP fibrillation on INS-1 cells but also promoted the cell growth. To characterize that the hIAPP-induced INS-1 cells death was weakened by Ru complexes directly, INS-1 cells were examined by phase contrast microscopy (**Figure S4**). Compared with healthy and regular shape in control cells, the cells after cultured with hIAPP appeared anomalous cellular morphology and lessened cell numbers. While after hIAPP co-treated with Ru complexes, the hIAPP-induced cell death and morphological changes were inhibited. To identify whether the Ru complexes could inhibit hIAPP-induced apoptosis, the caspase activity assay was conducted to analyze the activation of caspase-8 (Fas/TNF-mediated), caspase-9 (mitochondrial-mediated) and caspase-3 (executive caspase), which are vital components involved in extrinsic and intrinsic apoptotic signaling pathways³³. As shown in **Figure 6E**, hIAPP treatment significantly enhanced the activity of caspase-8 and caspase-9, and finally triggered the activity of executive caspase-3. Interestingly, the addition of Ru complexes markedly reversed the activation of caspase-8 and caspase-9, which irreversibly blocked the activity of caspase-3 in hIAPP-treated INS-1 cells. These results indicate that Ru complexes act as effective inhibitors for hIAPP-caused cell death.

Ru complexes inhibit hIAPP-induced ROS generation

Existing studies demonstrated that the mitochondrial dysfunction may lead to insulin secretory failure and metabolic dysregulation in T2DM^{41, 42}. Mitochondria are thought to be the principal source of ROS, whose ROS-signaling will enhance ROS production leading to potentially significant mitochondrial and cellular injury^{43, 44}. The ROS production has been highlighted as initiators for hIAPP-induced cell death in

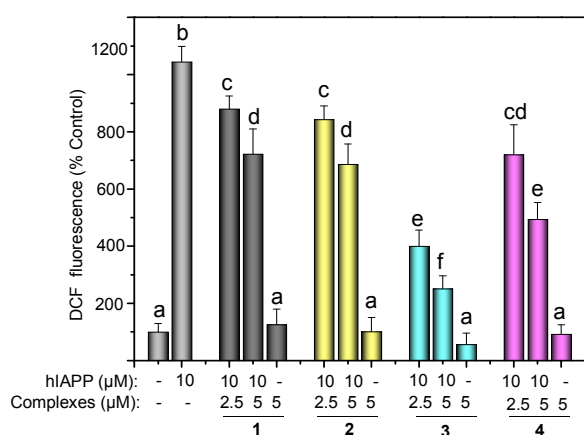


Figure 7. Ru complexes reduced ROS generation induced by hIAPP dose-dependently. INS-1 cells incubated hIAPP (10 μM) alone or with different Ru complexes (5 μM) at 37 °C for 60 min. Changes of ROS level was determined by DCF fluorescence intensity. The fluorescence intensity of control that treated without hIAPP and Ru complexes was expressed as 100%. The Values represented were means ±SD from three independent experiments. Bars with different characters are statistically different at $P < 0.05$ level as analyzed by one-way ANOVA multiple comparison.

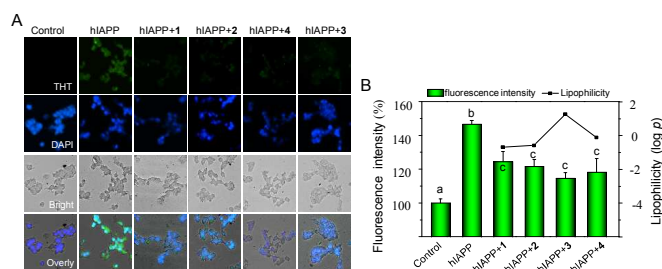


Figure 8. ThT fluorescence of hIAPP fibrillation inside INS-1 Cells. (A) INS-1 cells were pretreated with 10 μM hIAPP and 5 μM Ru complexes for 48 h at 37 °C, sequentially, ThT staining was used to examined the presence of intracellular hIAPP. The stained cells were visualized by fluorescence microscope. (B) ThT fluorescence intensity reflect the quantified evaluation of hIAPP aggregation. And the relationship between the ThT fluorescence and lipophilicity (logP) of complexes were also showed. Bars with different characters are statistically different at $P < 0.05$ level as analyzed by one-way ANOVA multiple comparison.

pancreatic beta cells⁴⁵⁻⁴⁷. To understand the biochemical and intracellular interaction between the Ru complexes and hIAPP deeply, the intracellular ROS level was monitored by detecting the intensity of fluorescein-labeled dye (H₂DCF-DA and DHE). The **Figure 7** showed the DCF fluorescence intensity as indicator of ROS generation that produced during hIAPP fibril formation with or without Ru complexes. After incubation of hIAPP, the intensity of the fluorescence was almost ten times higher than the control group. However, after co-treatment with Ru complexes, the ROS generation was reduced dose-dependently, implying that Ru complexes has disaggregated hIAPP amyloid fibril, thus suppressed the ROS formation. The same result was demonstrated in the DHE fluorescence assay (**Figure S5**), which was indicated that the superoxide anion induced by hIAPP in INS-1 cells were effectively inhibited by Ru complexes. Among these complexes, complex **3** achieved the best effect on inhibition of ROS generation. Therefore, Ru complexes, especially complex **3**, may exert protective effect

towards hIAPP-caused cell damage by restraining ROS generation.

Inhibition of hIAPP fibrillation inside INS-1 Cells by Ru complexes

Ru complexes showed inhibition in hIAPP caused cell damage, this is possible due to the intracellular hIAPP fibrillation were interfered by the Ru complexes. To conform whether the fibril disaggregation were still happened in INS-1 cells. The ThT fluorescence assay was carried out in INS-1 cells. As shown in **Figure 8A**, a strong and obvious green fluorescence were observed in cells when treated with hIAPP alone, when co-incubated with Ru complexes the ThT fluorescence intensity were decreased with only slight green fluorescence observed. Quantitative analysis of the fluorescence intensity was demonstrated in **Figure 8B**. Incubation of hIAPP alone increased the fluorescence intensity to 146.7%, which was decline to 118.4%, 121.5%, 114.7% and 123.2% after incubated with complexes **1**, **2**, **3** and **4** respectively, indicating that the hIAPP fibril formation was inhibited by the complexes. Obviously, the complex **3** showed a more effective in the inhibition. To further investigate the mechanism for this phenomenon that the complex **3** showed a more effective in the inhibition, the lipophilicity of complexes were investigated (**Figure 8B**). Several studies have showed that, the cellular uptake of Ru complexes was connected with their action of anticancer activities, which is thought to be a energy dependent and dependent on their lipophilicities^{48, 49}. Whether the lipophilicities of the Ru complexes in our study is proportional to their inhibition on hIAPP fibril formation is not yet clear. From the result, the complex **3** exhibited highest lipophilicity (logP = 1.27), which is consistent with its best inhibition on hIAPP fibril formation. Therefore, it is possible that, the high lipophilicity could enhance the cellular uptake of complex **3**, which in turn further increase the interaction of the complexes with hIAPP, thus inhibiting the formation of hIAPP fibril.

CONCLUSIONS

Recent studies have showed that the death of islet beta cells was due to the misfolding and hIAPP fibril formation in the pathogenesis of T2DM^{50, 51}. Thus, discovery of drugs that could inhibit the formation of amyloid fibrillation is thought to be a potentially therapeutic strategy towards diabetes. In this study, Ru complexes **1**, **2**, **3** and **4** were selected to investigate their influence on hIAPP fibrillation. Decreased Tyrosine intrinsic fluorescence and ThT fluorescence signal proved that hIAPP fibril formation was inhibited by Ru complexes. The following particle size analysis, AFM images and TEM images further indicated that the fibrillation of hIAPP was interrupted by Ru complexes to form nanoscale granular particles. This inhibition was revealed as a time dependently process. After that, we have found that Ru complexes could protect the INS-1 cells from hIAPP-caused cell damage by suppressing ROS generation during hIAPP fibrillation in cells and blocking of caspase activation and cell apoptosis. Moreover, the inhibition of hIAPP

fibril formation was discovered proportional to the lipophilicity of complexes. The complex with higher lipophilicity may showed more effective inhibition. Taken together, this study provides a strategy for design of Ru complexes for treatment of T2DM by targeting hIAPP.

Acknowledgements

This work was supported by National High Technology Research and Development Program of China (863 Program, SS2014AA020538), Science Foundation for Distinguished Young Scholars of Guangdong Province, Natural Science Foundation of China and Guangdong Province, Foundation for High-level Talents in Higher Education of Guangdong, Research Fund for the Doctoral Program of Higher Education of China (20114401110004), China Postdoctoral Science Foundation, Shenzhen Basic Research Grant (JCYJ20130401152508660) and YangFan Innovative & Entrepreneurial Research Team Project (201312H05).

Notes and references

Department of Chemistry, Jinan University, Guangzhou 510632, China. E-mail: tchentf@jnu.edu.cn., tlxlli@jnu.edu.cn.

* These authors contributed equally to the work.

† Electronic Supplementary Information (ESI) available: See DOI: 10.1039/b000000x/

- D. Eisenberg and M. Jucker, *Cell*, 2012, 148, 1188-1203.
- F. Chiti and C. M. Dobson, *Annu. Rev. Biochem.*, 2006, 75, 333-366.
- S. Laurent, M. R. Ejtehadi, M. Rezaei, P. G. Kehoe and M. Mahmoudi, *RSC Adv.*, 2012, 2, 5008-5033.
- P. Westermark, C. Wernstedt, E. Wilander, D. W. Hayden, T. D. O'Brien and K. H. Johnson, *Proc Natl Acad Sci U S A*, 1987, 84, 3881-3885.
- I. Saraogi, J. A. Hebda, J. Becerril, L. A. Estroff, A. D. Miranker and A. D. Hamilton, *Angew. Chem.*, 2010, 122, 748-751.
- R. L. Hull, G. T. Westermark, P. Westermark and S. E. Kahn, *J. Clin. Endocrinol. Metab.*, 2004, 89, 3629-3643.
- S. E. Kahn, D. A. D'Alessio, M. W. Schwartz, W. Y. Fujimoto, J. W. Ensnick, G. J. Taborisky and D. Porte, *Diabetes*, 1990, 39, 634-638.
- A. Lukinius, E. Wilander, G. Westermark, U. Engström and P. Westermark, *Diabetologia*, 1989, 32, 240-244.
- E. Ahmad, A. Ahmad, S. Singh, M. Arshad, A. H. Khan and R. H. Khan, *Biochimie*, 2011, 93, 793-805.
- J. R. Brender, S. Salamekh and A. Ramamoorthy, *Acc. Chem. Res.*, 2011, 45, 454-462.
- J. A. Hebda and A. D. Miranker, *Annu. Rev. Biophys.*, 2009, 38, 125-152.
- X. Li, L. Ma, W. Zheng and T. Chen, *Biomaterials*, 2014, 35, 8596-8604.
- T. A. Mirzabekov, M. C. Lin and B. L. Kagan, *J Biol Chem*, 1996, 271, 1988-1992.
- A. Quist, I. Doudevski, H. Lin, R. Azimova, D. Ng, B. Frangione, B. Kagan, J. Ghiso and R. Lal, *Proc Natl Acad Sci U S A*, 2005, 102, 10427-10432.
- X. Zhou, J. Tan, L. Zheng, S. Pillai, B. Li, P. Xu, B. Zhang and Y. Zhang, *RSC Adv.*, 2012, 2, 5418-5423.
- L. A. Scrocchi, Y. Chen, S. Waschuk, F. Wang, S. Cheung, A. A. Darabie, J. McLaurin and P. E. Fraser, *J Mol Biol*, 2002, 318, 697-706.
- K. Jeong, W. Y. Chung, Y. S. Kye and D. Kim, *Bioorg Med Chem*, 2010, 18, 2598-2601.
- R. Mishra, B. Bulic, D. Sellin, S. Jha, H. Waldmann and R. Winter, *Angew Chem Int Ed Engl*, 2008, 47, 4679-4682.
- B. Aliess, C. Hureau and P. Fallier, *Metallomics*, 2013, 5, 183-192.
- B. Ward, K. Walker and C. Exley, *J. Inorg. Biochem.*, 2008, 102, 371-375.
- V. B. Kenche, I. Zawisza, C. L. Masters, W. Bal, K. J. Barnham and S. C. Drew, *Inorg Chem*, 2013, 52, 4303-4318.
- T. Y. Lee, W. S. Chei, H. Ju, M. S. Lee, J. W. Lee and J. Suh, *Bioorg Med Chem Lett*, 2012, 22, 5689-5693.
- N. A. Vyas, S. S. Bhat, A. S. Kumbhar, U. B. Sonawane, V. Jani, R. R. Joshi, S. N. Ramteke, P. P. Kulkarni and B. Joshi, *Eur. J. Med. Chem.*, 2014, 75, 375-381.
- L. He, X. Wang, C. Zhao, H. Wang and W. Du, *Metallomics*, 2013, 5, 1599-1603.
- T. Chen, Y. Liu, W.-J. Zheng, J. Liu and Y.-S. Wong, *InCh*, 2010, 49, 6366-6368.
- G. Ramakrishna, D. A. Jose, D. K. Kumar, A. Das, D. K. Palit and H. N. Ghosh, *J. Phys. Chem. B*, 2005, 109, 15445-15453.
- C. Tan, S. Hu, J. Liu and L. Ji, *Eur. J. Med. Chem.*, 2011, 46, 1555-1563.
- Z. Luo, L. Yu, F. Yang, Z. Zhao, B. Yu, H. Lai, K.-H. Wong, S.-M. Ngai, W. Zheng and T. Chen, *Metallomics*, 2014.
- L. Li, Y.-S. Wong, T. Chen, C. Fan and W. Zheng, *Dalton T*, 2012, 41, 1138-1141.
- B.-w. Jing, W.-q. Wang, M.-h. Zhang and T. Shen, *Dyes and pigments*, 1998, 37, 177-186.
- W. Liu, X. Li, Y.-S. Wong, W. Zheng, Y. Zhang, W. Cao and T. Chen, *ACS nano*, 2012, 6, 6578-6591.
- T. Chen and Y.-S. Wong, *Biomed. Pharmacother.*, 2009, 63, 105-113.
- Y. Huang, L. He, W. Liu, C. Fan, W. Zheng, Y.-S. Wong and T. Chen, *Biomaterials*, 2013, 34, 7106-7116.
- L. He, Y. Huang, H. Zhu, G. Pang, W. Zheng, Y. S. Wong and T. Chen, *Adv. Funct. Mater.*, 2014, 24, 2737-2737.
- Y.-P. Yu, P. Lei, J. Hu, W.-H. Wu, Y.-F. Zhao and Y.-M. Li, *Chem. Commun.*, 2010, 46, 6909-6911.
- V. Pierroz, T. Joshi, A. Leonidova, C. Mari, J. Schur, I. Ott, L. Spiccia, S. Ferrari and G. Gasser, *J. Am. Chem. Soc.*, 2012, 134, 20376-20387.
- L. Ma, X. Li, Y. Wang, W. Zheng and T. Chen, *Int. J. Biochem. Cell Biol.*, 2014, 140, 143-152.
- Q. Ma, Y. Li, J. Du, H. Liu, K. Kanazawa, T. Nemoto, H. Nakanishi and Y. Zhao, *Peptides*, 2006, 27, 841-849.
- H. LeVine, 3rd, *Methods Enzymol*, 1999, 309, 274-284.
- F. H. Epstein, J. W. Höppener, B. Ahrén and C. J. Lips, *New Engl. J. Med.*, 2000, 343, 411-419.
- M. Bensellam, L. Van Lommel, L. Overbergh, F. Schuit and J.-C. Jonas, *Diabetologia*, 2009, 52, 463-476.
- H. Mulder and C. Ling, *Mol. Cell. Endocrinol.*, 2009, 297, 34-40.
- Q. Xie, L. He, H. Lai, W. Zheng and T. Chen, *RSC Adv.*, 2014, 4, 34210-34216.
- D. B. Zorov, M. Juhaszova and S. J. Sollott, *Biochim. Biophys. Acta.*, 2006, 1757, 509-517.
- X.-L. Li, G. Xu, T. Chen, Y.-S. Wong, H.-L. Zhao, R.-R. Fan, X.-M. Gu, P. C. Tong and J. C. Chan, *Int. J. Biochem. Cell Biol.*, 2009, 41, 1526-1535.
- L. Haataja, T. Gurlo, C. J. Huang and P. C. Butler, *Endocr. Rev.*, 2008, 29, 303-316.
- B. Konarkowska, J. F. Aitken, J. Kistler, S. Zhang and G. J. Cooper, *FEBS J.*, 2006, 273, 3614-3624.
- C. A. Puckett and J. K. Barton, *J. Am. Chem. Soc.*, 2007, 129, 46-47.
- Z. Zhao, Z. Luo, Q. Wu, W. Zheng, Y. Feng and T. Chen, *Dalton T*, 2014.
- J. W. Hoppener, B. Ahrén and C. J. Lips, *N Engl J Med*, 2000, 343, 411-419.
- J. W. Hoppener and C. J. Lips, *Int J Biochem Cell Biol*, 2006, 38, 726-736.